



You have downloaded a document from
RE-BUŚ
repository of the University of Silesia in Katowice

Title: Dielectric properties of bismuth ferrite-bismuth titanate ceramic composite

Author: Katarzyna Osińska, Agata Lisińska-Czekaj, Małgorzata Adamczyk, Dionizy Czekaj

Citation style: Osińska Katarzyna, Lisińska-Czekaj Agata, Adamczyk Małgorzata, Czekaj Dionizy. (2011). Dielectric properties of bismuth ferrite-bismuth titanate ceramic composite. "Archives of Metallurgy and Materials" Vol. 56 (4) (2011), s. 1093-1104. DOI: 10.2478/v10172-011-0122-9



Uznanie autorstwa - Użycie niekomercyjne - Bez utworów zależnych Polska - Licencja ta zezwala na rozpowszechnianie, przedstawianie i wykonywanie utworu jedynie w celach niekomercyjnych oraz pod warunkiem zachowania go w oryginalnej postaci (nie tworzenia utworów zależnych).



UNIWERSYTET ŚLĄSKI
W KATOWICACH



Biblioteka
Uniwersytetu Śląskiego



Ministerstwo Nauki
i Szkolnictwa Wyższego

K. OSIŃSKA*, A. LISIŃSKA-CZEKAJ*, H. BERNARD*, J. DZIK*, M. ADAMCZYK*, D. CZEKAJ*

DIELECTRIC PROPERTIES OF BISMUTH FERRITE – BISMUTH TITANATE CERAMIC COMPOSITE

WŁAŚCIWOŚCI DIELEKTRYCZNE KOMPOZYTÓW CERAMICZNYCH ŻELAZIANU BIZMUTU-TYTANIANU BIZMUTU

In this paper the $\text{BiFeO}_3/\text{Bi}_4\text{Ti}_3\text{O}_{12}$ (BF//BiT) ceramic-ceramic composites with 0-3 connectivity were prepared from BiFeO_3 and $\text{Bi}_4\text{Ti}_3\text{O}_{12}$ ceramic powders by free sintering method at $T=900^\circ\text{C}$, for different concentration of the BF ceramic phases. $\text{Bi}_4\text{Ti}_3\text{O}_{12}$ and BiFeO_3 ceramic powders were synthesized by the conventional mixed oxide method (MOM). Synthesized BF powder was dispersed in a BiT solution and next such composite was pressing and sintering. Crystalline structure was studied by X-ray diffraction method. The dielectric properties of the BF//BiT ceramic composites were also investigated. Temperature dependence of dielectric permittivity of BF//BiT composites was measured in the frequency range of $f=10\text{kHz}-100\text{kHz}$. It was found, that properties of the ceramic-ceramic composite are not a simple sum of properties of the phases constituting the composite but they depend on both the way of connectivity and mutual influence of the phases on each other. The abrupt increase in permittivity may indicate an excess of the percolation threshold, so the ceramic composite for the concentrations of the BF ceramic phase $c_V > 10\%$ cannot be indexed as composites with 0-3 connectivity.

Keywords: BiFeO_3 , $\text{Bi}_4\text{Ti}_3\text{O}_{12}$, composite, 0-3 connectivity

Kompozyty ceramiczno-ceramiczne $\text{BiFeO}_3/\text{Bi}_4\text{Ti}_3\text{O}_{12}$ (BF//BiT) o sposobie łączenia faz 0-3, dla różnej koncentracji fazy ceramicznej BF otrzymywano z proszków ceramicznych BiFeO_3 i $\text{Bi}_4\text{Ti}_3\text{O}_{12}$, metodą spiekania swobodnego w $T=900^\circ\text{C}$. Proszki ceramiczne $\text{Bi}_4\text{Ti}_3\text{O}_{12}$ i BiFeO_3 syntezowano metodą reakcji w fazie stałej z mieszaniny prostych tlenków. Zsyntezowany proszek ceramiczny BF zdyspergowano w roztworze BiT, a następnie otrzymany kompozyt prasowano i spiekano. Strukturę krystaliczną badano metodą dyfrakcji rentgenowskiej. Temperaturową zależność przenikalności elektrycznej kompozytów BF//BiT badano w zakresie częstotliwości $f=10\text{kHz}-100\text{kHz}$. Właściwości kompozytu ceramiczno-ceramicznego nie są prostą sumą właściwości poszczególnych faz składowych, ale stanowią efekt synergicznego oddziaływania faz składowych i sposobu ich wzajemnego połączenia. Gwałtowny wzrost wartości przenikalności dla 10%BF//BiT może świadczyć o przekroczeniu progu perkolacji, a więc kompozyty ceramiczno-ceramiczne BF//BiT o stężeniu ceramicznej fazy BF $c_V > 10\%$ nie mogą być indeksowane jako kompozyty o sposobie łączenia faz 0-3.

1. Introduction

Two-phase composites consist of a reinforcement and matrix. Newnham et al. established the notation for describing the number of dimensions that each phase is physically in contact with itself. To date, ten different types of two-phase electro composites have been studied: 0-0, 0-1, 0-2, 0-3, 1-1, 1-2, 1-3, 2-2, 2-3, 3-3 [1, 2]. In the case of electroceramic composites, the first number in the notation denotes the physical connectivity of the reinforcement phase and the second number refers to the physical connectivity of the matrix phase. The simplest types of composites are those with 0-3 connectivity.

Ceramic composites with 0-3 connectivity consist of three-dimensionally connected ceramic matrix loaded with active electroceramic particles. In 0-3 connectivity the connecting particles of first phase (reinforcement) are not in contact with each other and the second ceramic phase (matrix) is self-connected in all directions [3, 4].

In the present study BiFeO_3 (BF) ceramic phase are not in contact with each other (reinforcement) whereas $\text{Bi}_4\text{Ti}_3\text{O}_{12}$ (BiT) ceramic phase is self-connected in all directions (matrix).

Bismuth ferrite BiFeO_3 (BF) is a typical multiferroic material in which ferroelectricity and antiferromagnetism coexist at room temperature. Perovskite BiFeO_3 is ferroelectric ($T_C=830^\circ\text{C}$) and antiferromagnetic ($T_N=375^\circ\text{C}$). The high transition temperatures make this material of

* UNIVERSITY OF SILESIA, DEPARTMENT OF MATERIALS SCIENCE, 41-200 SOSNOWIEC, 2 ŚNIEŻNA STR., POLAND

particular interest for practical applications in devices based on the coupling of electrical and magnetic properties [5, 6].

Titanate bismuth $\text{Bi}_4\text{Ti}_3\text{O}_{12}$ (BiT) belongs to the Aurivillius compounds family that can be represented by the general formula: $(\text{Bi}_2\text{O}_2)^{2-}(\text{A}_{m-1}\text{B}_m\text{O}_{3m+1})^{2+}$. For BiT: $\text{A}=\text{Bi}$, $\text{B}=\text{Ti}$ and $m=3$. $\text{Bi}_4\text{Ti}_3\text{O}_{12}$ high Curie temperature ($T_C=670^\circ\text{C}$) gives it wide applicability in electronic elements, as transducers, piezoelectric and memory devices [7, 8].

In the present study attention is confined to one of the most commonly encountered connectivity 0-3. The $\text{BiFeO}_3/\text{Bi}_4\text{Ti}_3\text{O}_{12}$ (BF//BiT) ceramic composites exhibiting the 0-3 connectivity, with different concentration of BF ceramic phases, has been fabricated on the base BiFeO_3 and $\text{Bi}_4\text{Ti}_3\text{O}_{12}$ ceramic powders by the free sintering method at $T=900^\circ\text{C}$. Results of influence of the BF ceramic phase on microstructure, crystalline structure and dielectric properties of ceramic composite with volume fraction of the BF phase from $c_V=2\%$ up to $c_V=20\%$ are also reported.

2. Experimental

In the present work the $\text{BiFeO}_3/\text{Bi}_4\text{Ti}_3\text{O}_{12}$ ceramic composites of volumetric content $c_V=2\%$, 4% , 6% , 8% , 10% , 16% and 20% and 0-3 connectivity were prepared from BF and BiT ceramic powders in the form of disks.

BiFeO_3 ceramic powder was obtained by the mixed oxide method (MOM) from stoichiometric mixture of bismuth (III) oxide Bi_2O_3 (Aldrich, 99.9%) and iron (III) oxide Fe_2O_3 (Aldrich, 99%) as starting materials according to the formula:



The powders were synthesized at temperature $T=750^\circ\text{C}$ for $t=10\text{h}$.

The synthesis of $\text{Bi}_4\text{Ti}_3\text{O}_{12}$ ceramic powders, at temperature $T=1000^\circ\text{C}$ for $t=3\text{h}$, was performed according to the formula:



from the stoichiometric mixture of bismuth oxide Bi_2O_3 (99.9% ALDRICH) and titanium oxide TiO_2 (99.9% POCH) by the standard mixed oxide method (MOM). After synthesis the samples of BF and BiT were powdered by ball-milling in liquid medium and dried. Synthesized BF powder was dispersed in a BiT solution and next such composite was pressed at $p=600\text{MPa}$ and sintered at temperature $T=900^\circ\text{C}$ for $t=3\text{h}$.

Apparent density of the sintered samples was measured by the Archimedes method. The specimens were 91-96% of the density calculated from X-ray diffraction pattern for all compositions.

The crystal structure was examined by X-ray diffraction with CoK_α radiation (θ - 2θ method, scan step size $\Delta\theta=0.02$ deg, scan type continuous, scan step time $t=4\text{s}$) at room temperature. The lattice parameters for $\text{Bi}_5\text{Ti}_3\text{FeO}_{15}$, $\text{Bi}_6\text{Ti}_3\text{Fe}_2\text{O}_{18}$, $\text{Bi}_7\text{Ti}_3\text{Fe}_3\text{O}_{21}$, BiFeO_3 and $\text{Bi}_4\text{Ti}_3\text{O}_{12}$ ceramic specimens were calculated using Rietveld refinement, embedded into the computer program PowderCell 2.4 [9].

For electric measurements, composite samples were covered with silver paste electrodes. The dielectric properties of BF//BiT composites were studied with the impedance gain/phase analyser HP4192A in the frequency range from $f=10\text{kHz}$ to $f=100\text{kHz}$. The measurements were performed with heating from $T=0^\circ\text{C}$ to $T=750^\circ\text{C}$ at a rate of $1\text{deg}/\text{min}$.

3. Results

The dependence of apparent density on concentration of BF ceramic phase for BF//BiT composites is given in Fig.1. One can see from Fig. 1 that addition of BF component in amount of $c_V=2\%$ increases the apparent density of the composite for about $c_V=6\%$, next apparent density decreased.

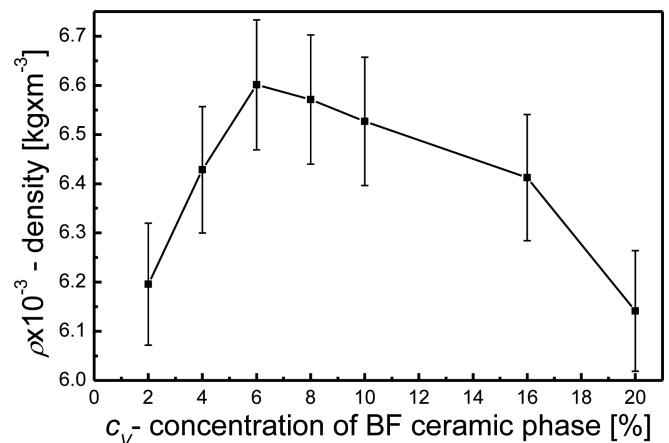


Fig. 1. Dependence of apparent density of BF//BiT composite on concentration of BF ceramic phase

X-ray diffraction patterns of BF//BiT composites are given in Fig. 2-Fig. 8. Comparison of X-ray diffraction patterns of BF//BiT composites are in Fig. 9. One can see, that for $c_V=2$ - 10% of BF ceramic phase all diffraction data showed the existence of two phases: $\text{Bi}_5\text{Ti}_3\text{FeO}_{15}$ and $\text{Bi}_4\text{Ti}_3\text{O}_{12}$. The $\text{Bi}_5\text{Ti}_3\text{FeO}_{15}$ performed according to the formula:

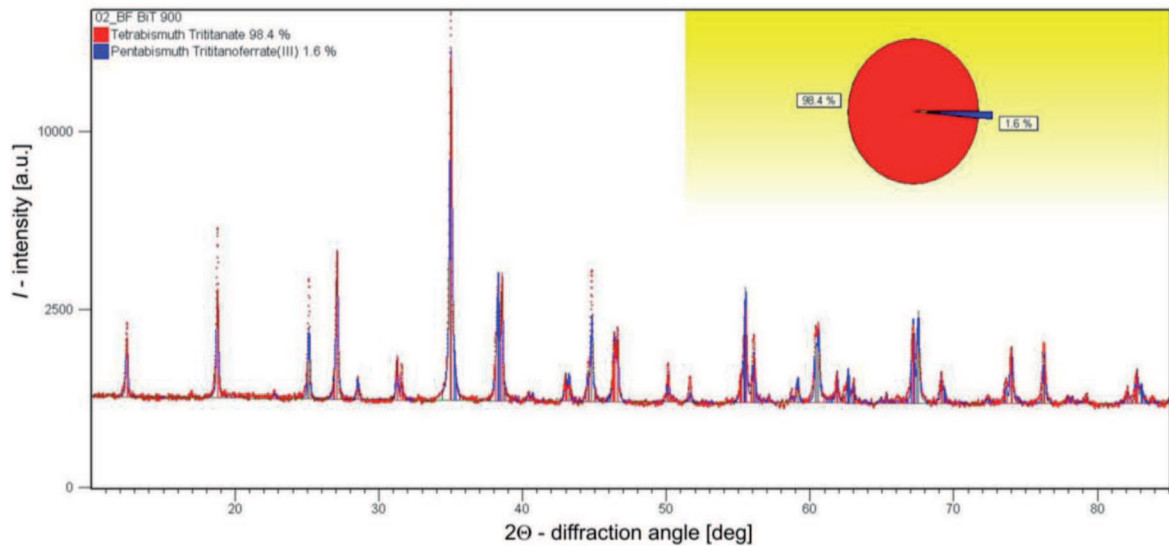


Fig. 2. X-ray diffraction patterns of 2%(BF-BiT)//BiT composite

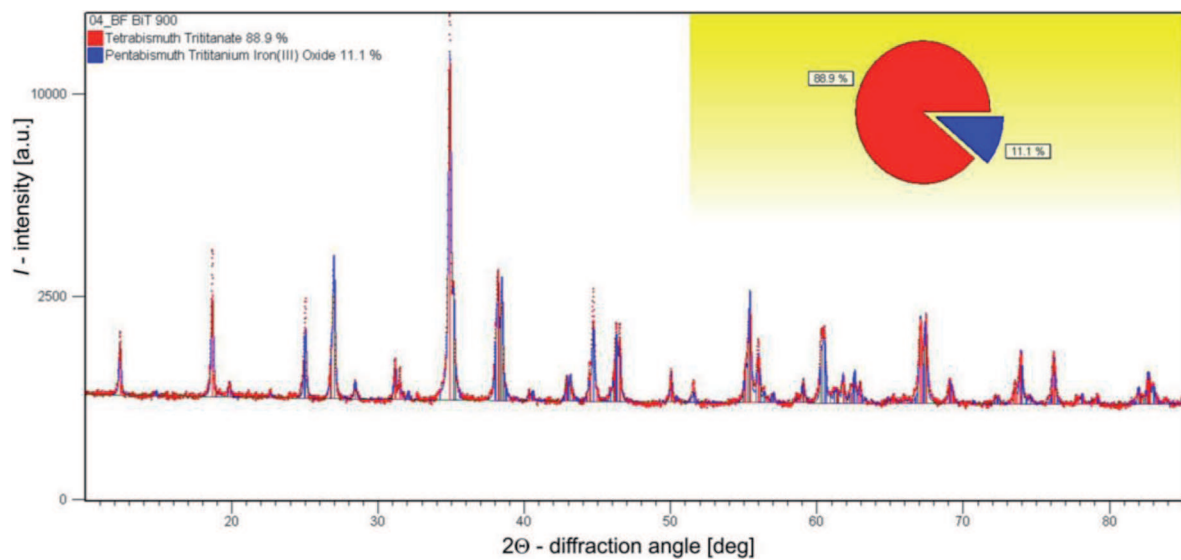


Fig. 3. X-ray diffraction patterns of 4%(BF-BiT)//BiT composite

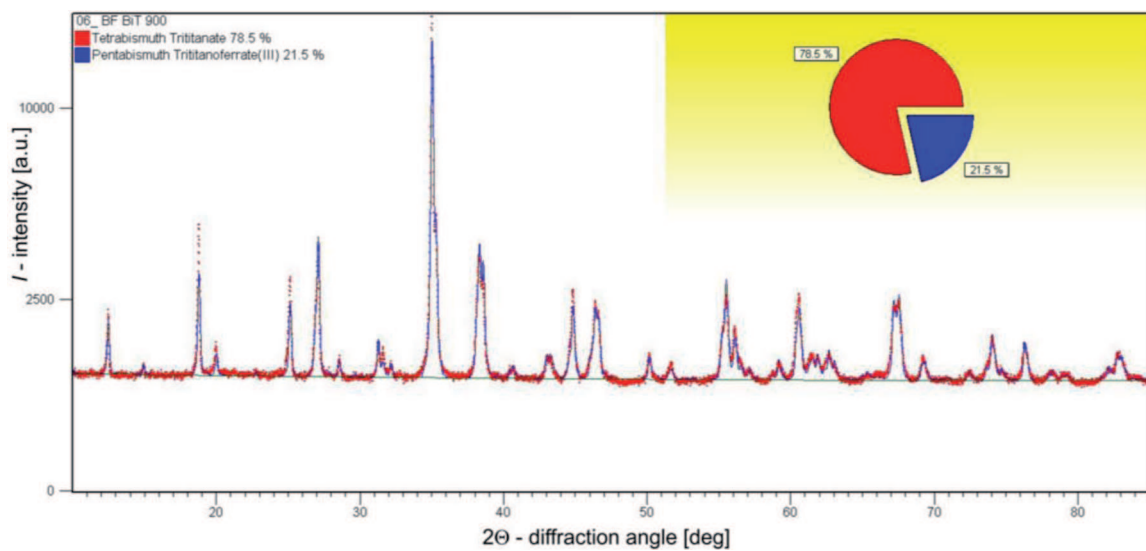


Fig. 4. X-ray diffraction patterns of 6%(BF-BiT)//BiT composite

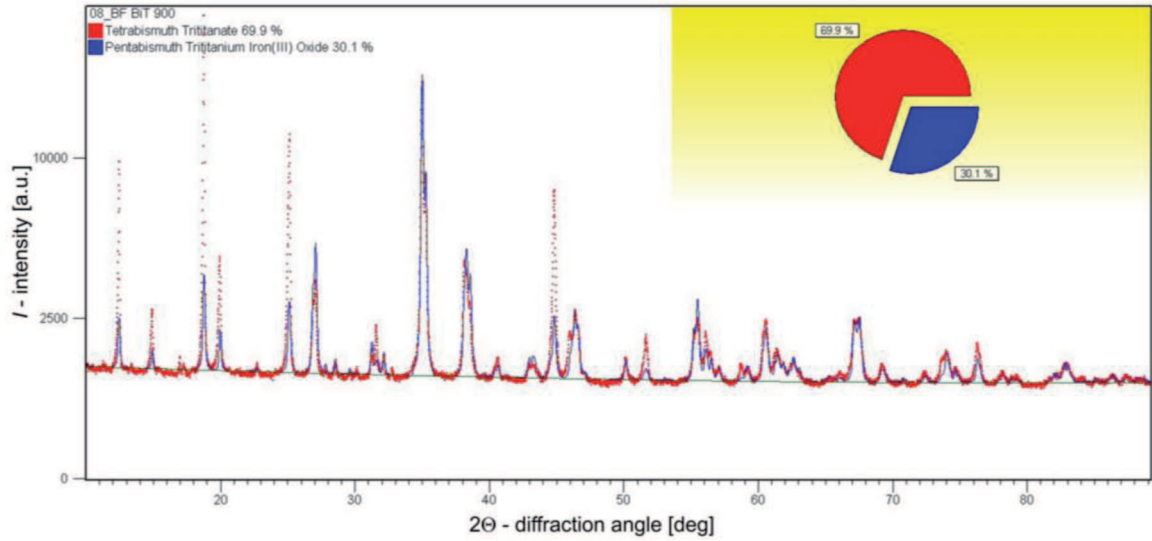


Fig. 5. X-ray diffraction patterns of 8%(BF-BiT)//BiT composite

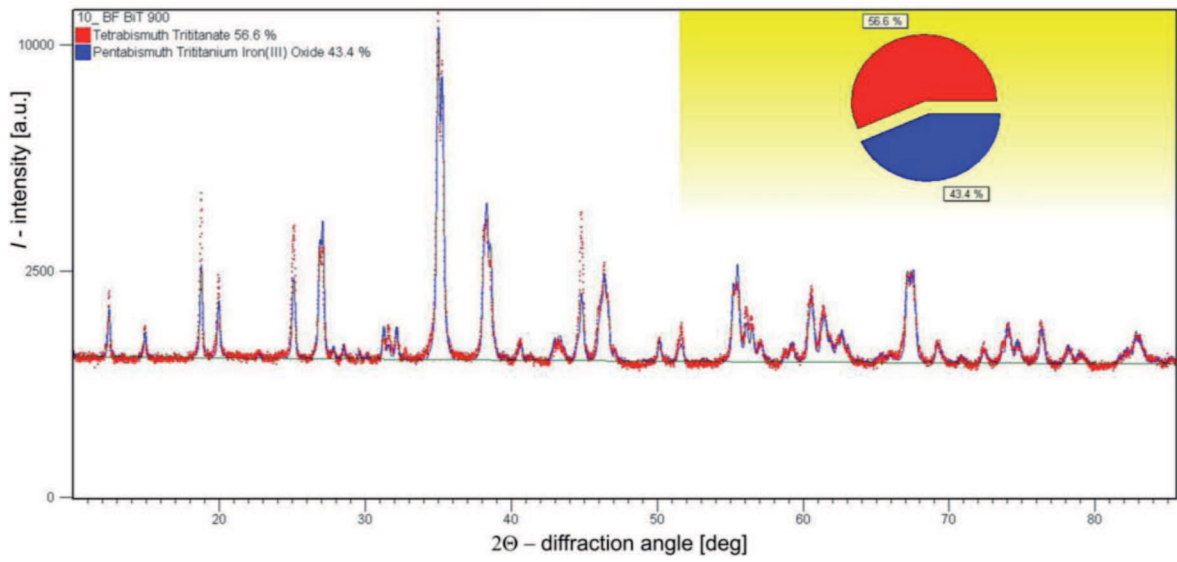


Fig. 6. X-ray diffraction patterns of 10%(BF-BiT)//BiT composite

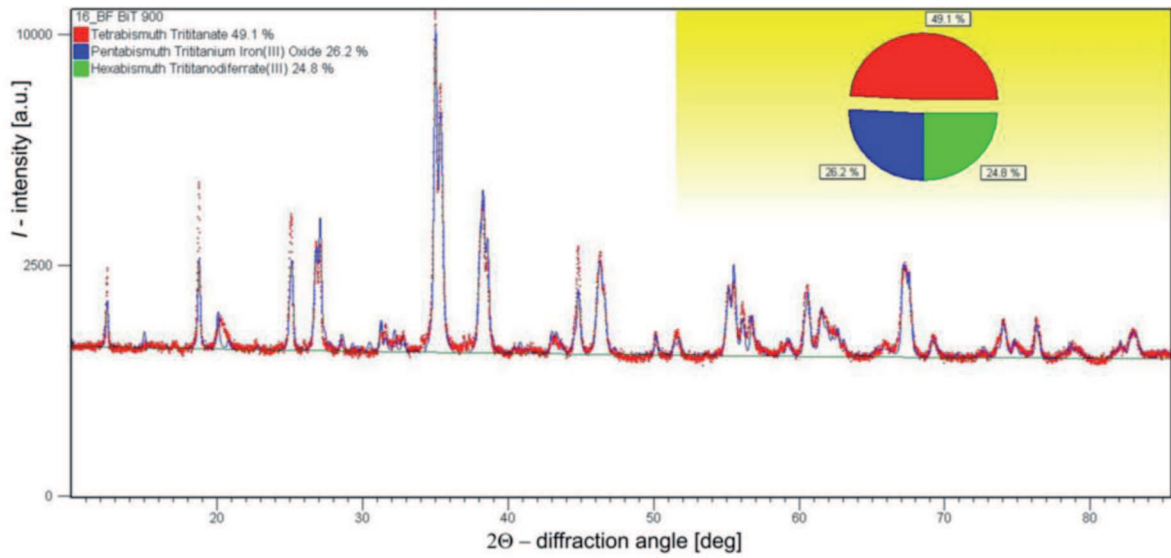


Fig. 7. X-ray diffraction patterns of 16%(BF-BiT)//BiT composite

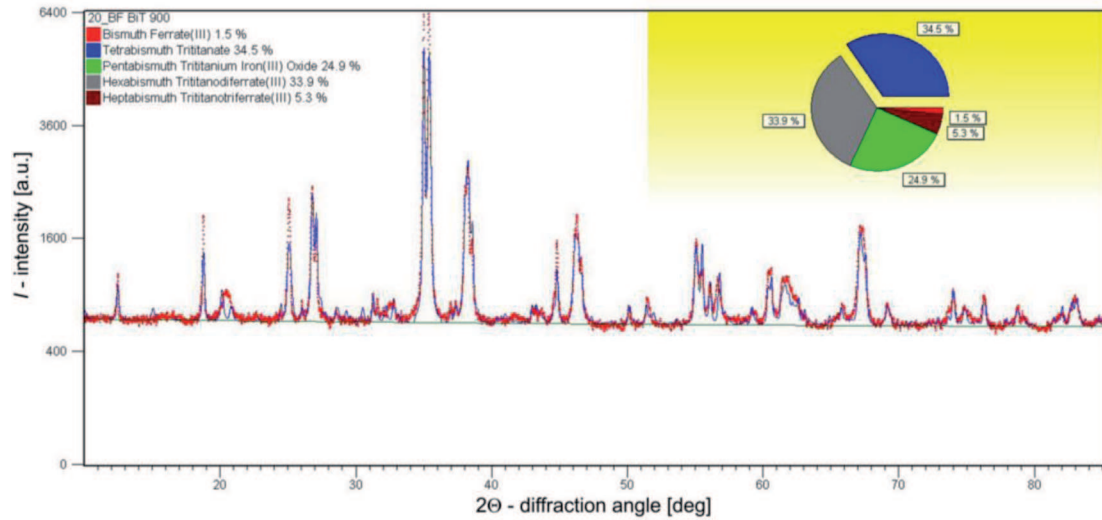


Fig. 8. X-ray diffraction patterns of 20%(BF-BiT)//BiT composite

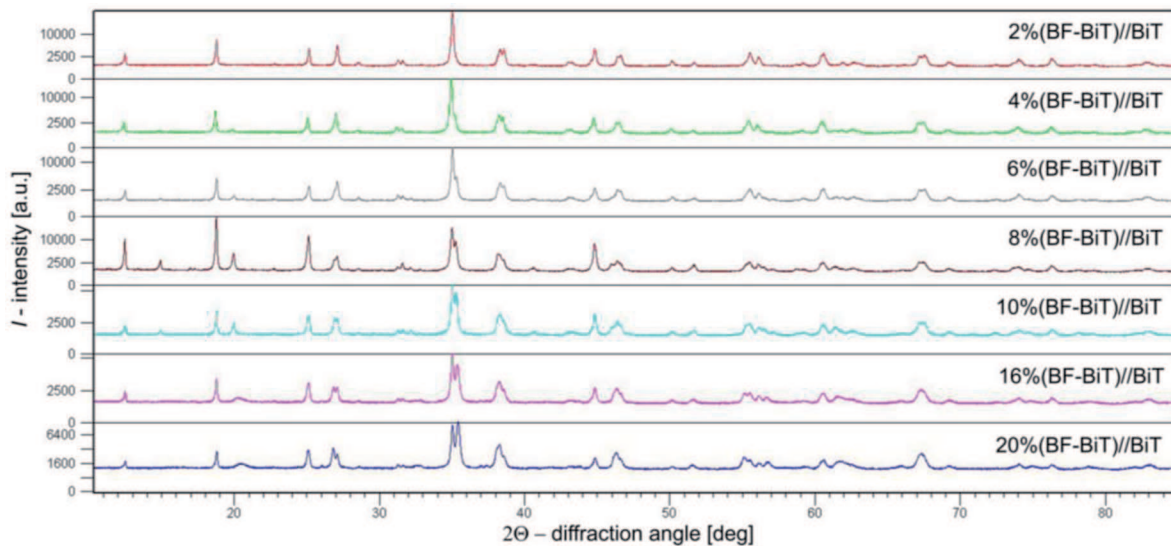
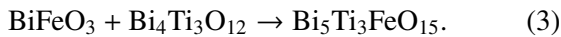
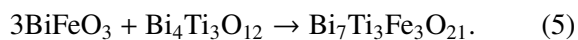
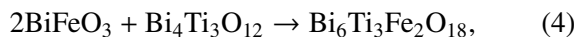


Fig. 9. Comparison of X-ray diffraction patterns of BF//BiT composites



For $c_V=16\%$ of BF ceramic phase we observed existence of three phases: $\text{Bi}_5\text{Ti}_3\text{FeO}_{15}$, $\text{Bi}_6\text{Ti}_3\text{Fe}_2\text{O}_{18}$, $\text{Bi}_4\text{Ti}_3\text{O}_{12}$ and for $c_V=20\%$ - five phases: $\text{Bi}_5\text{Ti}_3\text{FeO}_{15}$, $\text{Bi}_6\text{Ti}_3\text{Fe}_2\text{O}_{18}$, $\text{Bi}_7\text{Ti}_3\text{Fe}_3\text{O}_{21}$, BiFeO_3 and $\text{Bi}_4\text{Ti}_3\text{O}_{12}$. The $\text{Bi}_6\text{Ti}_3\text{Fe}_2\text{O}_{18}$ and $\text{Bi}_7\text{Ti}_3\text{Fe}_3\text{O}_{21}$ performed according to the formulas:



As a result of the reaction of BiT and BF formed different ceramic phases, therefore, in the rest of the work uses the model generated a following entry of ceramic composites: (BF-BiT)//BiT. Parameters of X-ray analysis of (BF-BiT)//BiT composites are given in Tab.1.

The dominating phase, as it should have been expected, was $\text{Bi}_4\text{Ti}_3\text{O}_{12}$ phase which adopted the monoclinic symmetry described well with $P1c1(7)$ space group. The structures of $\text{Bi}_5\text{Ti}_3\text{FeO}_{15}$, $\text{Bi}_6\text{Ti}_3\text{Fe}_2\text{O}_{18}$, $\text{Bi}_7\text{Ti}_3\text{Fe}_3\text{O}_{21}$ were found as orthorhombic (space group $Fmm2(42)$) and the BiFeO_3 assigned hexagonal structure with $R3c(161)$ space group.

Parameters of X-ray analysis of (BF-BiT)//BiT composites

Concentration of BF ceramic phase c_V [%]		2		4		6	
		$\text{Bi}_5\text{Ti}_3\text{FeO}_{15}$	$\text{Bi}_4\text{Ti}_3\text{O}_{12}$	$\text{Bi}_5\text{Ti}_3\text{FeO}_{15}$	$\text{Bi}_4\text{Ti}_3\text{O}_{12}$	$\text{Bi}_5\text{Ti}_3\text{FeO}_{15}$	$\text{Bi}_4\text{Ti}_3\text{O}_{12}$
Calculated density $\rho \times 10^{-3}$ [kg/m ³]		8.037	8.051	8.062	8.056	8.056	8.049
Apparent density $\rho \times 10^{-3}$ [kg/m ³]		6.196		6.483		6.601	
Space group		<i>Fmm2</i> (42)	<i>P1c1</i> (7)	<i>Cmc21</i> (36)	<i>P1c1</i> (7)	<i>Fmm2</i> (42)	<i>P1c1</i> (7)
Elementary cell parameters	a_0 [nm]	4.121	1.663	4.115	1.662	0.544	1.663
	b_0 [nm]	0.544	0.541	0.544	0.541	4.113	0.541
	c_0 [nm]	0.547	0.545	0.547	0.544	0.547	0.545
	α [°]	90	90	90	90	90	90
	β [°]	90	99.35	90	99.34	90	99.35
	γ [°]	90	90	90	90	90	90
	$V \times 10^6$ [pm ³]	1226.65	483.24	1222.92	482.91	1223.68	483.36
Rietveld analysis parameters	R_{exp} [%]	3.74		3.74		3.10	
	R_p [%]	6.36		5.28		4.52	
	R_{wp} [%]	9.06		7.20		6.09	

Concentration of BF ceramic phase c_V [%]		8		10	
		$\text{Bi}_5\text{Ti}_3\text{FeO}_{15}$	$\text{Bi}_4\text{Ti}_3\text{O}_{12}$	$\text{Bi}_5\text{Ti}_3\text{FeO}_{15}$	$\text{Bi}_4\text{Ti}_3\text{O}_{12}$
Calculated density $\rho \times 10^{-3}$ [kg/m ³]		8.052	8.048	8.051	8.048
Apparent density $\rho \times 10^{-3}$ [kg/m ³]		6.571		6.527	
Space group		<i>Cmc21</i> (36)	<i>P1c1</i> (7)	<i>Cmc21</i> (36)	<i>P1c1</i> (7)
Elementary cell parameters	a_0 [nm]	4.115	1.662	4.116	1.663
	b_0 [nm]	0.544	0.541	0.544	0.541
	c_0 [nm]	0.547	0.545	0.547	0.545
	α [°]	90	90	90	90
	β [°]	90	99.33	90	99.33
	γ [°]	90	90	90	90
	$V \times 10^6$ [pm ³]	1224.35	483.42	1224.51	483.42
Rietveld analysis parameters	R_{exp} [%]	2.84		3.01	
	R_p [%]	11.55		5.27	
	R_{wp} [%]	20.50		7.95	

Concentration of BF ceramic phase c_V [%]		16		
		$\text{Bi}_5\text{Ti}_3\text{FeO}_{15}$	$\text{Bi}_6\text{Ti}_3\text{Fe}_2\text{O}_{18}$	$\text{Bi}_4\text{Ti}_3\text{O}_{12}$
Calculated density $\rho \times 10^{-3}$ [kg/m ³]		8.074	8.047	8.048
Apparent density $\rho \times 10^{-3}$ [kg/m ³]		6.412		
Space group		<i>Cmc</i> 21(36)	<i>Fmm</i> 2(42)	<i>P1c</i> 1(7)
Elementary cell parameters	a_0 [nm]	4.096	0.547	1.663
	b_0 [nm]	0.545	4.945	0.541
	c_0 [nm]	0.547	0.549	0.545
	α [°]	90	90	90
	β [°]	90	90	99.33
	γ [°]	90	90	90
	$V \times 10^6$ [pm ³]	1221.02	1483.33	483.43
Rietveld analysis parameters	R_{exp} [%]	2.97		
	R_p [%]	5.42		
	R_{wp} [%]	7.33		

Concentration of BF ceramic phase c_V [%]		20				
		BiFeO_3	$\text{Bi}_5\text{Ti}_3\text{FeO}_{15}$	$\text{Bi}_6\text{Ti}_3\text{Fe}_2\text{O}_{18}$	$\text{Bi}_7\text{Ti}_3\text{Fe}_3\text{O}_{21}$	$\text{Bi}_4\text{Ti}_3\text{O}_{12}$
Calculated density $\rho \times 10^{-3}$ [kg/m ³]		8.352	8.082	8.058	7.991	8.047
Apparent density $\rho \times 10^{-3}$ [kg/m ³]		6.141				
Space group		<i>R3c</i> (161)	<i>Fmm</i> 2(42)	<i>Fmm</i> 2(42)	<i>Fmm</i> 2(42)	<i>P1c</i> 1(7)
Elementary cell parameters	a_0 [nm]	0.558	0.545	0.547	0.545	1.663
	b_0 [nm]	0.558	4.084	4.941	5.895	0.541
	c_0 [nm]	1.385	0.548	0.548	0.546	0.545
	α [°]	90	90	90	90	90
	β [°]	90	90	90	90	99.34
	γ [°]	120	90	90	90	90
	$V \times 10^6$ [pm ³]	373.12	1219.78	1481.25	1753.54	483.46
Rietveld analysis parameters	R_{exp} [%]	3.66				
	R_p [%]	5.50				
	R_{wp} [%]	7.49				

Dependence of the real part of dielectric permittivity ε' (a) and the loss tangent $\text{tg}\delta$ (b) on temperature for $\text{Bi}_4\text{Ti}_3\text{O}_{12}$ electroceramic used for composite fabrication is given in Fig. 10. It can be seen from Fig. 10 that with increased frequency decreasing the maximum value of real part permittivity ε'_m and decreasing temperature of the phase transition.

Temperature dependence of the real part permittivity ε' (a) and the loss tangent $\text{tg}\delta$ (b) of (BF-BiT)//BiT composites with different concentrations of ceramics phase for $f=20\text{kHz}$ and for $f=100\text{kHz}$ are shown in Fig. 11 and

Fig. 12, respectively. The permittivity ε' of BiT ceramic is higher in comparison with that of the (BF-BiT)//BiT composites for $f=100\text{kHz}$.

Fig. 13 shows the dependence of the real part of permittivity ε'_m (a) and corresponding temperature T'_m (b) on the volume fraction of the BF-BiT ceramic phase for (BF-BiT)//BiT composite at $f=100\text{kHz}$. One can see that the ε'_m and corresponding temperature T'_m of the (BF-BiT)//BiT composites increases with an increase in the volume fraction of the BF-BiT ceramic phase to $c_V=10\%$ and next decreases.

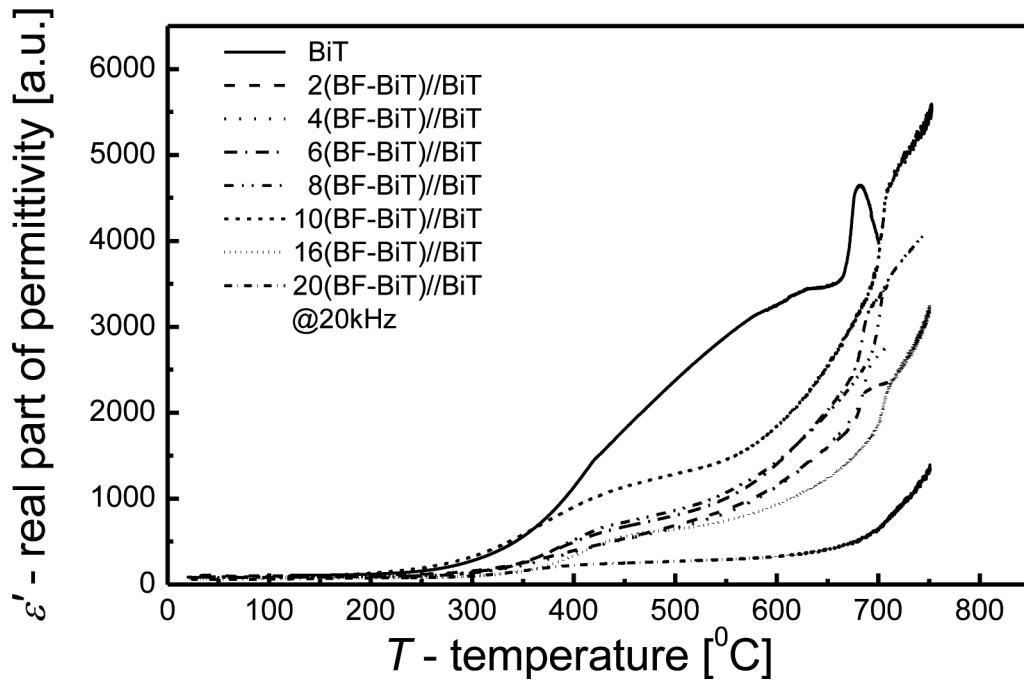


Fig. 10a. Temperature dependence of the real part of dielectric permittivity ϵ' for BiT ceramic at $f=10\text{kHz}$, $f=20\text{kHz}$ and $f=100\text{kHz}$

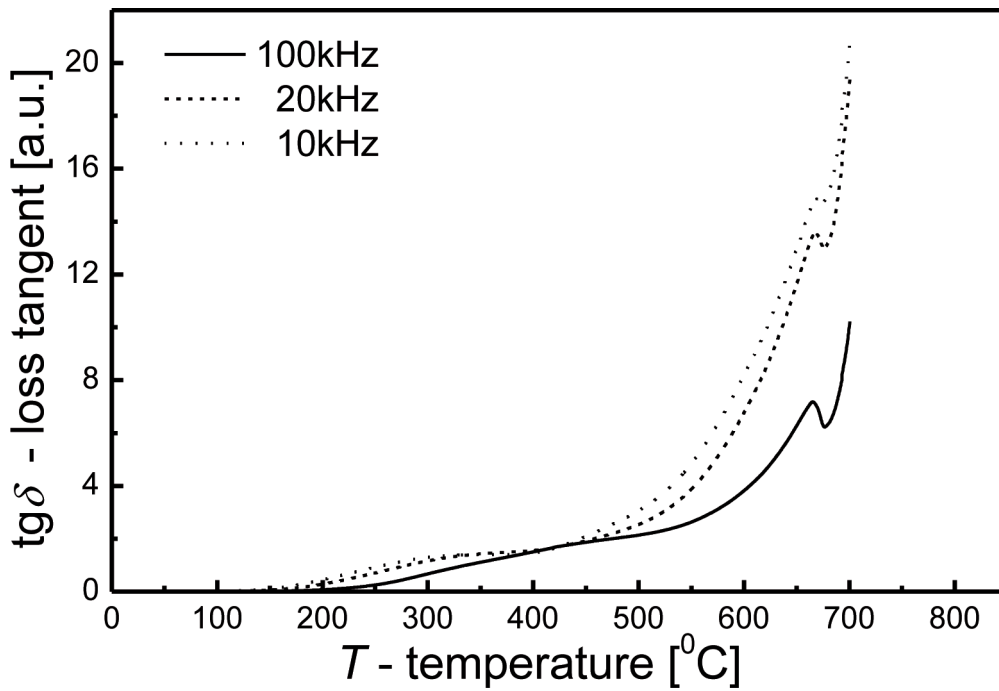


Fig. 10b. Temperature dependence of the loss tangent $\text{tg}\delta$ for BiT ceramic at $f=10\text{kHz}$, $f=20\text{kHz}$ and $f=100\text{kHz}$

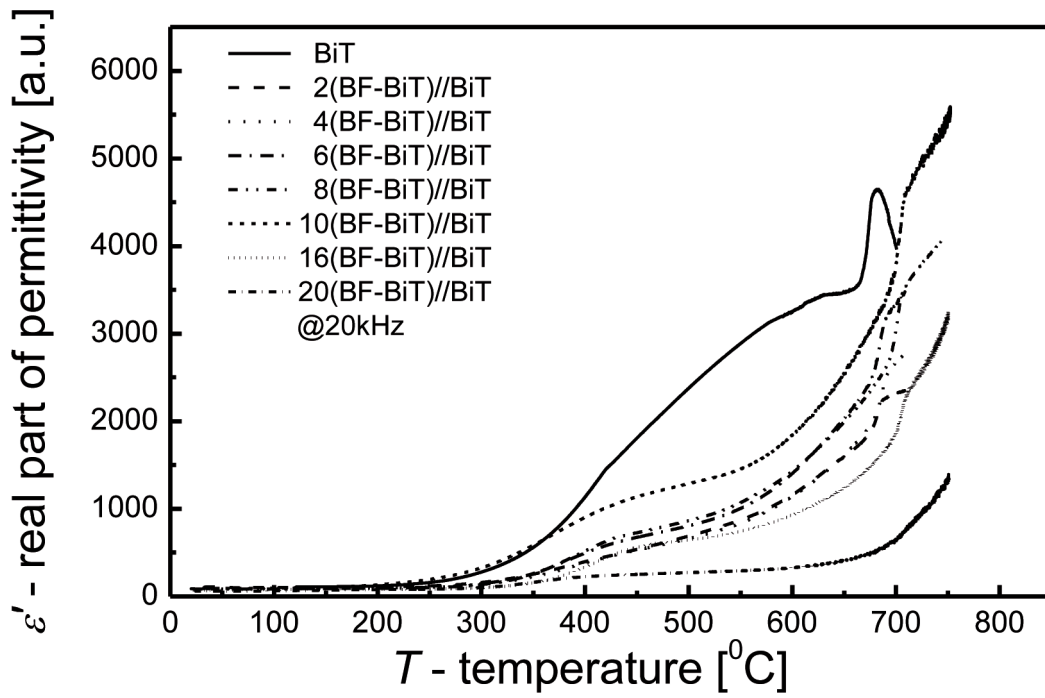


Fig. 11a. Temperature dependence of the real part permittivity ε' of (BF-BiT)//BiT composites with different concentrations of ceramics phase for $f=20\text{kHz}$

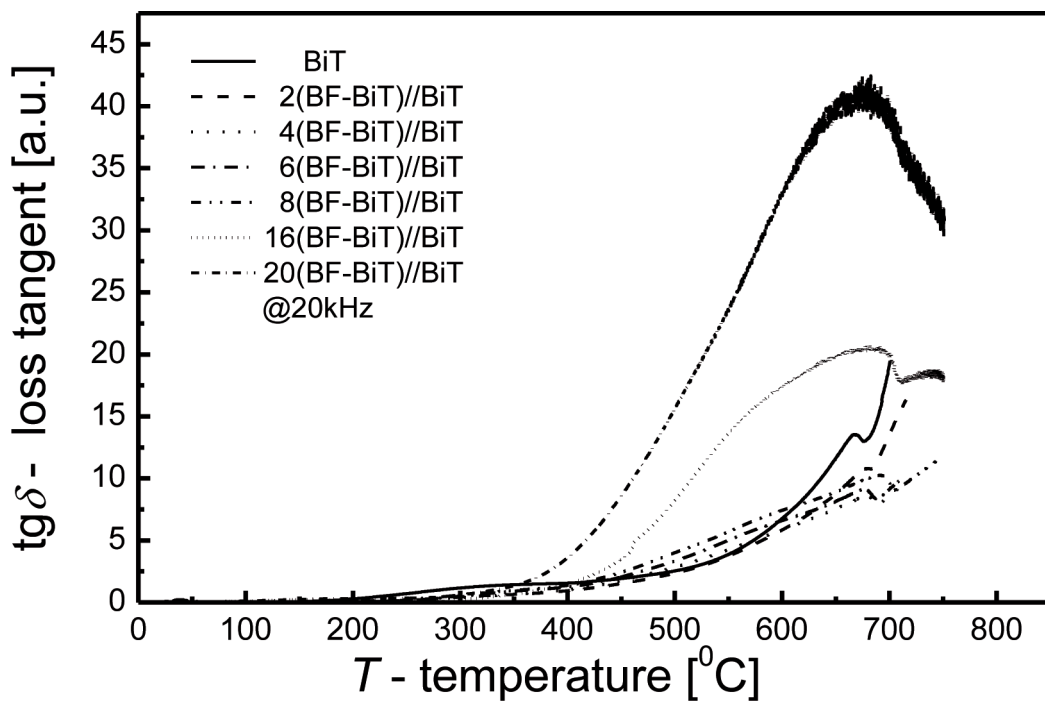


Fig. 11b. Temperature dependence of the loss tangent $\text{tg}\delta$ of (BF-BiT)//BiT composites with different concentrations of ceramics phase for $f=20\text{kHz}$

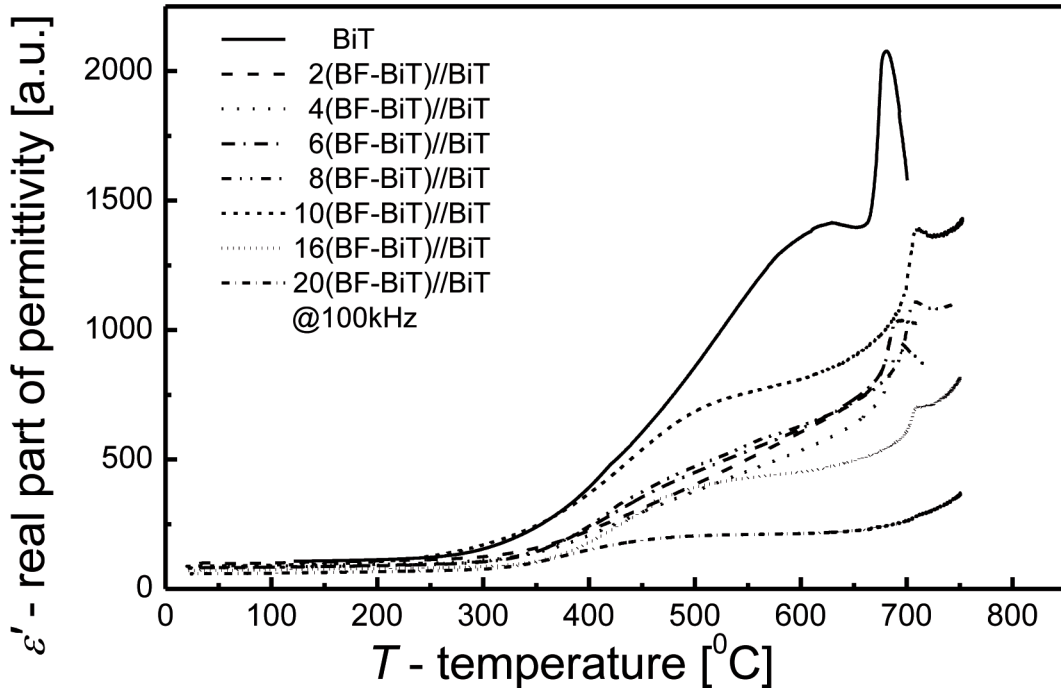


Fig. 12a. Temperature dependence of the real part permittivity ϵ' of (BF-BiT)//BiT composites with different concentrations of ceramics phase for $f=100\text{kHz}$

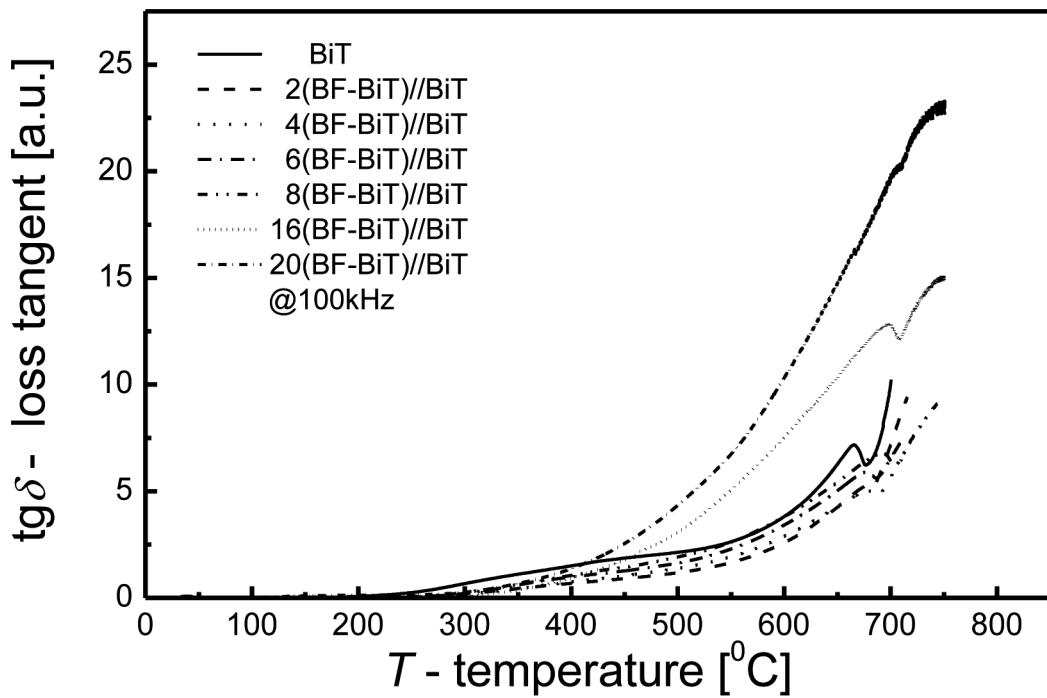


Fig. 12b. Temperature dependence of the loss tangent $\text{tg}\delta$ of (BF-BiT)//BiT composites with different concentrations of ceramics phase for $f=100\text{kHz}$

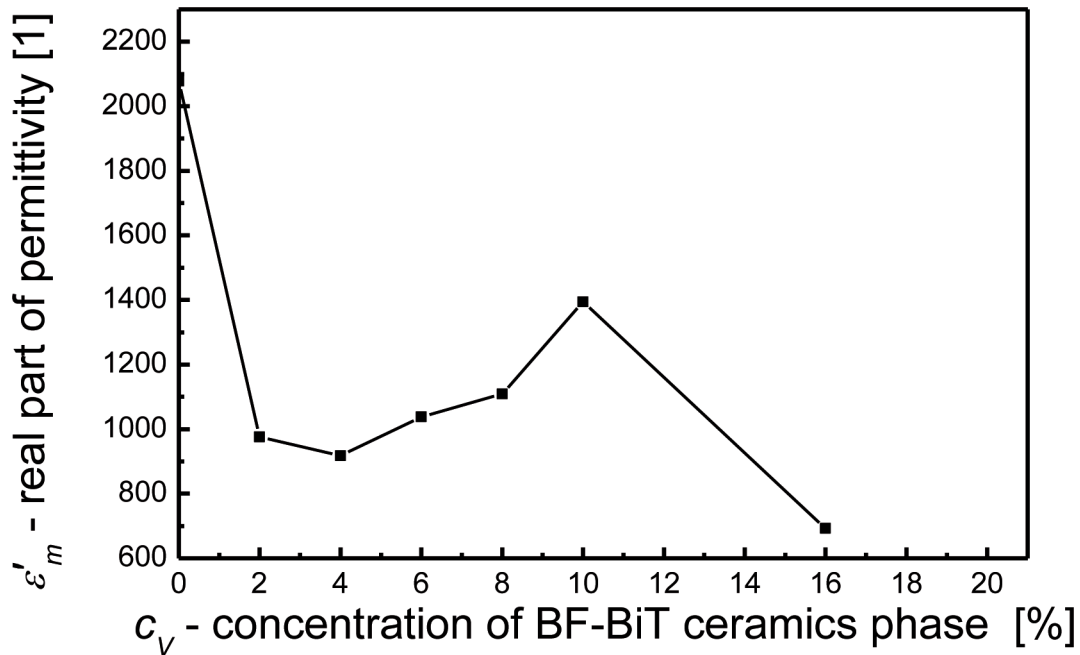


Fig. 13a. Dependence of the real part of dielectric permittivity ϵ'_m on the volume fraction of the BF-BiT ceramic phase for (BF-BiT)//BiT composite at $f=100\text{kHz}$

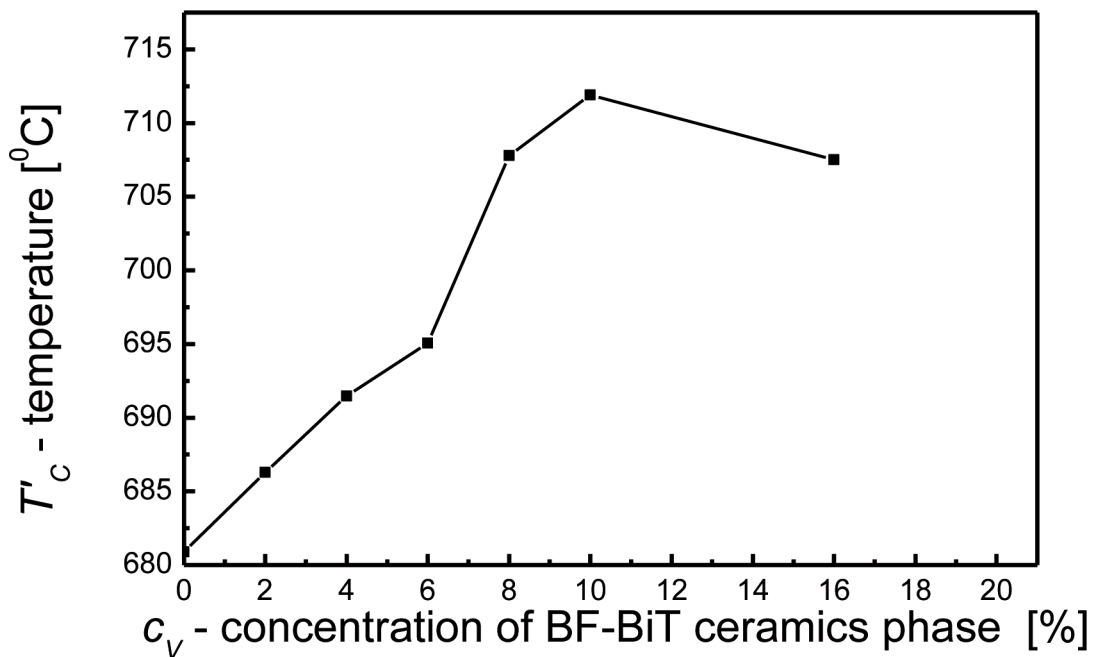


Fig. 13b. Dependence of the temperature T'_m on the volume fraction of the BF-BiT ceramic phase for (BF-BiT)//BiT composite at $f=100\text{kHz}$

It is worth noting that the abrupt increase in dielectric permittivity has been observed in the (BF-BiT)//BiT ceramic composite with concentration of the active ceramic phase $c_v \leq 10\%$. It can be explained in the terms of percolation threshold. It is commonly known [9] that the percolation threshold may vary depending upon the matrix and dopant chemistries, particle sizes, shapes and spatial orientation as well as process-

ing parameters. In case of high amounts of active ceramic phases in the ceramic composite it is possible that the percolation limit of the composite (in terms of the BF-BiT ceramic particles) may have been reached at this volume fraction. The direct conduction paths of ceramic material has been formed all the way both the top and bottom electrode of the pellet-like composite samples.

4. Conclusions

In the present study we have fabricated the electroactive ceramic composites of 0-3 connectivity using BiFeO_3 and $\text{Bi}_4\text{Ti}_3\text{O}_{12}$ ceramic powder by free sintering method. Temperature of the real part of permittivity and loss tangent for ceramic composites with 0-3 connectivity show that dielectric properties are determined by the BF-BiT ceramic phase (even at $c_V \sim 2\%$). The abrupt increase in permittivity may indicate an excess percolation threshold, so the ceramic-polymer composite for concentration of the active ceramic phase $c_V > 10\%$ cannot be indexed as composites with 0-3 connectivity.

Acknowledgements

The present research has been supported by Polish Ministry of Education and Science from the funds for science in 2008-2011 as a research project N N507 446934.

REFERENCES

- [1] K. Osińska, M. Adamczyk, D. Czekaj, Prace Komisji Nauk Ceramicznych-Polski Biuletyn Ceramiczny, *Ceramika* **101**, 125-131 (2008).
- [2] R.E. Newnham, D.P. Skinder, L.E. Cross, *Materials Research Bulletin* **13**(5), 325-336 (1978).
- [3] K. Osińska, M. Adamczyk, D. Czekaj, Prace Komisji Nauk Ceramicznych- Polski Biuletyn Ceramiczny, *Ceramika* **103**, 245-252 (2008).
- [4] K. Osińska, M. Adamczyk, M. Parcheniak, D. Czekaj, *Archives of Metallurgy and Materials* **54**, 985-997 (2009).
- [5] M. Mahesh Kumar, V.R. Palkar, K. Srinivas, S.V. Suryanarayana, *Applied Physics Letters* **76**, 19, 2764-2776 (2000).
- [6] Y.P. Wang, L. Zhou, M.F. Zhang, X.Y. Chen, J.-M. Liu, Z.G. Liu, *Applied Physics Letters* **84**, 10, 1731-1733 (2004).
- [7] L. Zhang, R. Chu, S. Zhao, G. Li, Q. Yin, *Materials Science and Engineering B* **116**, 99-103 (2005).
- [8] H. Bernard, J. Dzik, A. Lisińska-Czekaj, K. Osińska, D. Czekaj, *Inżynieria Materiałowa* **178**, 6 1404-1408 (2010).
- [9] G. Nolze, W. Kraus, *Powder Diffraction, Journal of Applied Crystallography* **13**, 256 (1998).